# Effect of Sterilization on Protein Adsorption of Micro- and Nano-sized Aluminum Hydroxide Adjuvant

Damai Ria Setyawati[1(✉)], Sjaikhurrizal El Muttaqien[1], Donny Ramadhan[2], and Etik Mardliyati[1]

[1] Research Center for Vaccine and Drugs Development, National Research and Innovation Agency (BRIN), Jakarta, Indonesia
dama004@brin.go.id

[2] Research Center for Pharmaceutical Ingredients and Traditional Medicine, National Research and Innovation Agency (BRIN), Jakarta, Indonesia

**Abstract.** Aluminum hydroxide (AH) is one of the aluminum-based adjuvants that forms needle-like crystalline structure with the average particle size of 1–20 μm. Due to their favorable safety profile, AH adjuvant has been used widely in various human vaccine in diphtheria, tetanus, pertussis, hepatitis, and papilloma virus vaccines. The antigen-adjuvant interaction is strongly governed by the adjuvant's physicochemical characters, such as shape, dimension and surface charge. Based on this concept, tremendous efforts to amplify the performance of the adjuvant have been made by modifying its particle size into nano-sized adjuvant. Also, during vaccine formulation, several physical processes may take place and potentially affect the antigen-adjuvant interaction, such as dilution, salt and aging exposure, pH change, heat, pressure and shear forces stress. Therefore, in this study we have examined the effect of sterilization and pH of AH nanoparticle (AHNp) with the average size of ~160 nm on its physical characterization and adjuvant-antigen interaction. The obtained results were compared with those from AH microparticle (AHMp) and commercial AH adjuvant (AHC).

AHMp and AHNp were prepared by using common precipitation method through the addition of alkali to the solution of aluminum chloride. The aluminum content of both AH suspension is 12.1 mg/mL. The average particle size of AHMp and AHNp by static light scattering are 4.21 μm and 0.16 μm, respectively. For evaluating the effect of autoclave on AH properties, all AH samples on glass container were autoclaved at 121 °C for 30 dan 60 min. The result shows that all samples did not give significant physical character change after autoclave. All measured parameters including the solid content of AH suspension, the acquired mass after freezing dry, pH value, and visual appearance remained the same as those before autoclave. The X-ray diffractogram of AHMp and AHNp revealed that the diffraction bands were sharper after autoclaving.

Following autoclaving, all fraction of (bovine serum albumin) BSA added into the adjuvant could be completely adsorbed by AHNp, AHMp, and AHC samples, as high as its pre-autoclaved condition, achieving maximum adsorption capacity. Such phenomena could be obtained even when volume ratio of adjuvant/BSA multiplied 20-times. It indicates that the binding efficiency BSA to all adjuvant


I. Nurlaila et al. (Eds.): ICHR 2022, AHSR 56, pp. 824–832, 2023.
https://doi.org/10.2991/978-94-6463-112-8_75

samples was not affected by the autoclaving in all given test condition. On the other hand, the pH of AH suspension significantly affects the protein adsorption capacity. The highest binding efficiency of AH-protein could be achieved in physiological pH condition, highlighting the pH-dependency of AH-protein interaction.

**Keywords:** adjuvant · aluminum hydroxide · adsorption · sterilization

## 1 Introduction

An effective vaccine usually comprised of both antigen and adjuvant to provide long term protection against infection. Antigen is required to elicit specific immune response while adjuvant is needed to boost the obtained host immune response against the antigen. Aluminum hydroxide (AH) is one of the aluminum-based adjuvants that forms needle-like crystalline structure with the average particle size of 1–20 μm [1]. Due to their favorable safety profile, AH adjuvant has been used widely in various human vaccine in diphtheria, tetanus, pertussis, hepatitis, and papilloma virus vaccines. Several mechanisms of immunopotentiation by aluminum-containing adjuvants have been proposed, including as antigen depot for providing gradual release of the antigen in the injection site, as a facilitator for presenting the antigen to antigen-presenting cells, and as an immunostimulator for recruiting various subsets of immunocompetent cells to release inflammatory cytokines [2].

The interaction of antigen and adjuvant is strongly governed by the adjuvant's physicochemical characters, such as shape, dimension and surface charge. Based on this concept, tremendous efforts to amplify the performance of the adjuvant have been made by modifying its particle size into nano-sized adjuvant [3]. From our previous report, a stabilized AH nanoparticle (AHNp) with the average size of ~ 200 nm exhibited stronger immunopotentiation activity of purified DENV3 pre–Membrane Envelope (prM-E) recombinant protein than those of micro-sized counterpart (AHMp) without altering its intrinsic toxicity profile [4][5]. Besides the aforementioned parameters, the binding of protein and adjuvant has been intensively studied to establish the optimum condition of adjuvant-antigen interaction which is contribute directly to the immune-enhancing effect. The adsorption of antigen onto adjuvant heavily depends on pH-dependent electrostatic force between them which is represented by the isoelectric point (iep) value of each component. At neutral pH, AH adjuvant (iep = 9 .6) is positively charged, therefore, it is important to select negatively charged antigen at pH 7.4 to ensure the optimum ionic interaction between the antigen and the adjuvant [6].

During vaccine formulation, several physical processes may take place, such as dilution, salt and aging exposure, pH change, heat, pressure and shear forces stress, and it potentially affect the antigen-adjuvant interaction [7]. Burrell and Coworkers have reported that autoclaving commercial AH adjuvant (AHC) increased the degree of crystallinity and importantly reduced its antigen adsorption capacity [8]. Therefore, in this study we have examined the effect of sterilization and the pH change of AHNp on its physical characterization and adjuvant-antigen interaction and compare the obtained result with those from AHMp and AHC.

## 2 Materials and Methods

The AHMp and AHNP were prepared by reacting aluminum chloride with sodium hydroxide, as previously reported [9]. AHC (Alhydrogel®) was purchased from InvivoGen (Frederikssund, Denmark). Phosphate-buffered saline (PBS) pH 7.4 was prepared by dissolving one PBS Tablet from Merck in 200 mL of deionized water, yielding 0.01 M phosphate buffer, 0.0027 M potassium chloride and 0.137 SM sodium chloride, pH 7.4. Particle size distribution of all samples was measured by static light scattering (Horiba LA95A).

The protein adsorption test was conducted using established protocol [10]. Briefly, stock solutions of BSA were prepared in 10 mM PBS (pH 7.4) buffer. The suspension of AH sample was mixed with BSA solution and incubated for 1 h in room temperature using rotary shaker incubator. After incubation, the mixture was centrifuged at 13,000 rpm for 15 min. The supernatant was assayed for protein concentration by bicinchoninic acid assay (BCA) test through measuring the absorbance at 562 nm.

## 3 Results and Discussion

In this study, AHmp was prepared by using common precipitation method through the addition of alkali to the solution of aluminum chloride. The reaction product formed fluffy and flocculent aluminum hydroxide precipitate called crystalline aluminum oxyhydroxide [AlO(OH)] with the particle size ranged from 1.98–15.17 μm, and average particle size of 4.21 μm (Fig. 1a). Various attempts to improve the AH adjuvant activity by downsizing its particle size into nano-sized particle have been made through different methods, including sonication step [11, 12], microfluidizer [13], hydrothermal process [14, 15], and high shear homogenization [9], with the obtained particle size ranged from around 50 to 200 nm. In this research, we applied high-speed homogenization towards homogeneous AHmp suspension to generate AHnp. As the AHmp suspension is sensitive to shear, the applied high shear force could breakdown the size of the micro-crystal clusters into its nano-sized particle with the average size of 160 nm (Fig. 1b) and narrow particle size range. The individual micro-crystals aggregates, however, could still be observed in the AHnp suspension, forming larger cluster. On the other hand, AHc showed a homogeneous particle which consisted of large clusters of primary crystallites with diameter of 4.02 μm. This result is comparable with the previous work that revealed the majority of the particle size of AHc ranged from 2.20–3.30 μm [16]. Morphologically, AH adjuvant composed of a very small fiber particle having dimensions on the order of nanometers that tend to form larger assemblies due to the weak intermolecular bonds between the hydroxyl groups [17, 18]. The formed aggregates, however, is readily to be redispersed into smaller fragment uniformly after mixing.

For evaluating the effect of autoclave on AH properties, all AH samples on glass container were autoclaved at 121 °C for 30 dan 60 min. The result shows that all samples did not give significant physical character change after autoclave. For each corresponding sample, all measured parameters including the solid content of AH suspension, the acquired mass after freezing dry, and visual appearance remained relatively the same as those before autoclave, as shown Table 1 and Fig. 2. The pH value of the AHMp- and

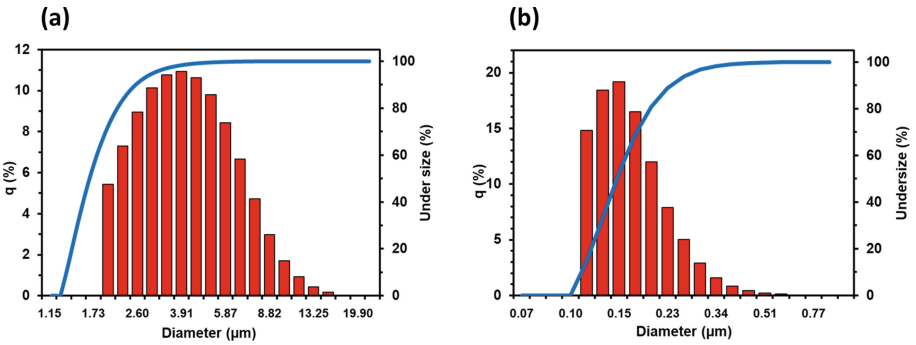


**Fig. 1.** Particle size distribution (red bar) and its cumulative undersize (blue line) of (a) AHMp and (b) AHNp measured by static light scattering

**Table 1.** Sample characterization

| Sample | pH | Total solid (%) | Weight after freezing dry 1 mL suspension (mg) |
|---|---|---|---|
| AHMp | 6.68 | 1.37 | 20.00 |
| AHMp-autoclave | 6.35 | 1.27 | 24.62 |
| AHNp | 7.88 | 1.56 | 22.60 |
| AHNp-autoclave | 7.81 | 1.05 | 23.20 |
| AHC | 6.49 | 0.40 | 9.72 |
| AHC-autoclave | 6.55 | 0.39 | 10.00 |

AHNp-autoclaved samples was slightly lower compared to those before autoclave, while those of autoclaved AHC increased. The decrease of pH after autoclave is because of the deprotonation and dehydration process of AH that took place through the additional double hydroxide bridges of the AH during the heat exposure [19].

For chemical characterization, the content of aluminum in AHnp and AHmp measured by XRF analysis was 12.1 mg/mL suspension, while those of AHc was 4.3 mg/mL. For further evaluation, the AHnp and AHmp suspensions was diluted to achieve similar aluminum concentration with those of AHc.

AH adjuvant is crystalline aluminum oxyhydroxide which the crystallinity is in the middle of the reported range of boehmite samples [18]. The thermal and pressure exposure during the autoclave process may affect the degree of crystallinity of AH. As shown in Fig. 3, the XRD patterns of all AH adjuvants tested are similar although with different intensities. The patterns of specific crystalline phase of AH adjuvants are identified by d-spacing at around 6.46, 3.18, 2.35, 1.86, and 1.44 Å. Importantly, autoclave process did not produce any significant change of crystallinity of AHC. However, both AHMp and AHNp showed sharper diffraction bands after autoclaving, revealing their higher crystallinity compared to those before autoclave. This X-ray diffractogram of both AHMp and AHNp is in accordance with their pH change in Table 1; the slight pH reduction of

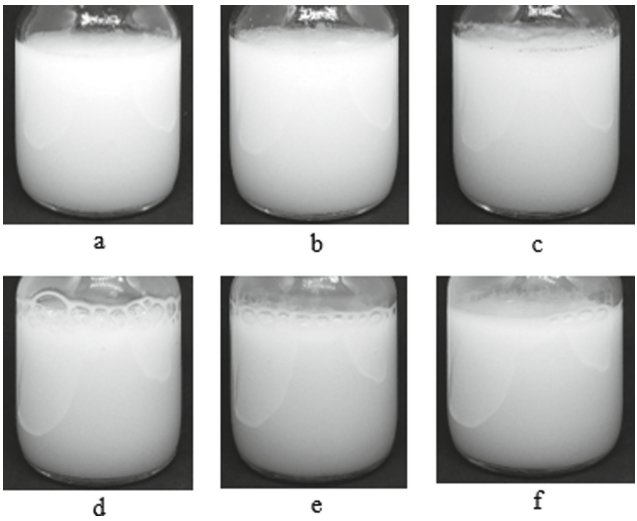


**Fig. 2.** Visual observation of AHMp (a-c) and AHNp (d-f). Key: before autoclave (a,d); after 30 min autoclave (b,e); and after 60 min autoclave (c,f)

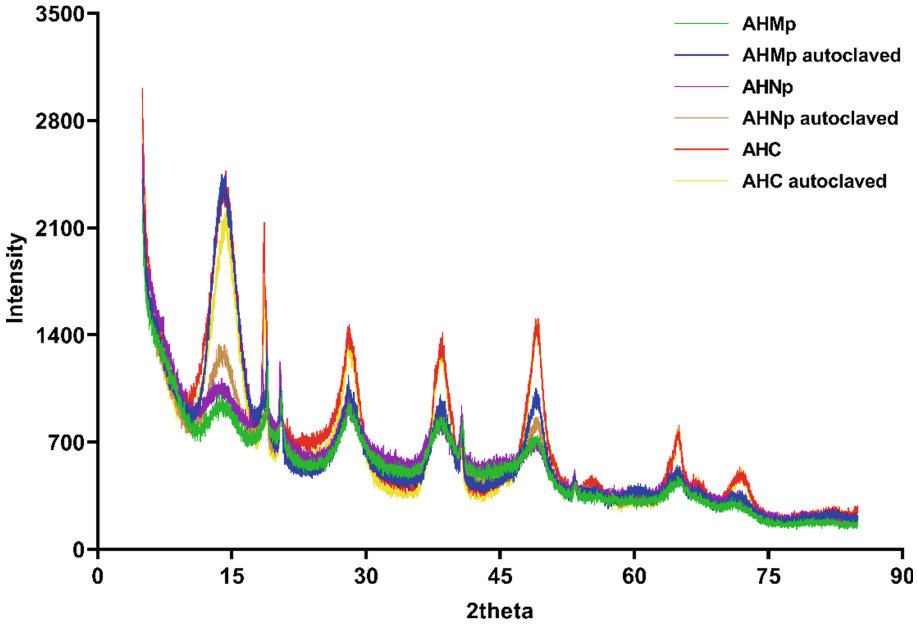


**Fig. 3.** The X-ray diffractogram of all AH adjuvant, before and after 30 min autoclave

AHMp and AHNp after autoclave implied both AHs crystal became more highly ordered due to the deprotonation and dehydration reaction during autoclave.

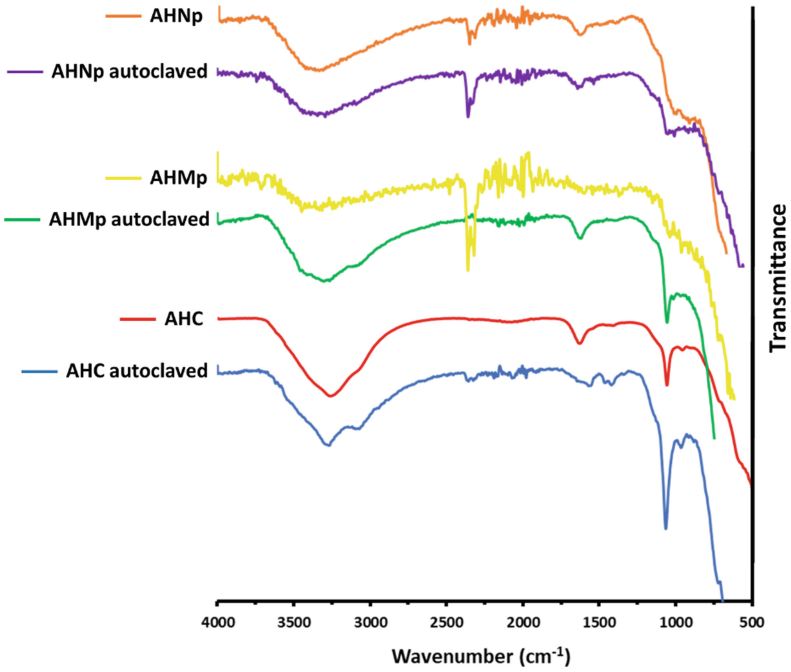


**Fig. 4.** FTIR spectra of all AH adjuvant, before and after 30 min autoclave

From FTIR spectra in the 500–4000 $cm^{-1}$ region, all samples displayed major bands at 3700–2700, 1640, and 1100 $cm^{-1}$ (Fig. 4). The wide strong band at 3700–2700 $cm^{-1}$ is assigned to OH-stretching from both hydroxyl group and absorbed water, while the band at 1640 $cm^{-1}$ is the HOH-bending band of adsorbed water only. The bands at 1065 and 3098 $cm^{-1}$ are associated with structural hydroxyl environments of poorly crystalline boehmite [6]. It is known that a gradual increase in intensities of FTIR spectra band may indicate the increase of crystallinity of the sample [15]. However, the change of crystallinity of AHMp and AHNp in response to autoclave process could not be observed from this FTIR result.

The amount of antigen adsorbed onto the adjuvant is critical as it determines the immunogenicity of the vaccine. To further evaluate the effect of autoclave on antigen adsorption, adsorption capacity was measured by directly mixing bovine serum albumin (BSA) solution with an aqueous suspension of AH sample. The BSA (iep = 4.8) was selected as protein model in the adsorption test due to its negative charge at neutral pH. At the physiological pH, the negatively charged BSA is expected to interact with the positive charge of AH. In the first adsorption test, the concentration of BSA solution added to the adjuvant solution was set as 2 mg/mL while the volume ratio of adjuvant/BSA was varied from 1:1 to 1:20 (v/v). Following autoclaving, all fraction of BSA added into the adjuvant could be completely adsorbed by AHnp, AHmp, and AHc samples, as high as its pre-autoclaved condition, achieving maximum adsorption capacity (Table 2). Such phenomena could be obtained even when the volume ratio of adjuvant/BSA multiplied 20-times. At this highest volume ratio (1:20), the concentration of AH sample was diluted

**Table 2.** The effect of volume ratio of adjuvant/BSA (2 mg/mL) on adsorbed protein

| Sample | Adsorbed BSA (%) | | | | |
|---|---|---|---|---|---|
| | volume ratio 1:1 | volume ratio 1:2.5 | volume ratio 1:5 | volume ratio 1:9 | volume ratio 1:20 |
| AHC | 101.96 | 102.29 | 104.40 | 100.03 | 103.15 |
| AHMp | 100.46 | 101.71 | 104.32 | 100.53 | 102.87 |
| AHMp-30 min autoclave | 100.53 | 101.60 | 104.32 | 99.09 | 103.09 |
| AHMp-60 min autoclave | 100.36 | 101.79 | 104.35 | 99.28 | 102.96 |
| AHNp | 100.57 | 102.24 | 104.38 | 100.07 | 103.07 |
| AHNp-30 min autoclave | 100.61 | 102.29 | 104.38 | 100.34 | 102.79 |
| AHNp-60 min autoclave | 100.63 | 102.46 | 104.38 | 100.20 | 102.68 |

**Table 3.** The effect of BSA concentration on adsorbed protein (1/1 (*v/v*))

| Sample | Adsorbed BSA (%) | | | | |
|---|---|---|---|---|---|
| | BSA conc. 2 mg/mL | BSA conc. 3 mg/mL | BSA conc. 6 mg/mL | BSA conc. 10 mg/mL | BSA conc. 20 mg/mL |
| AHC | 101.96 | 101.93 | 68.90 | 100.66 | 17.88 |
| AHMp | 100.46 | 101.68 | 101.03 | 99.45 | 15.93 |
| AHMp-30 min autoclave | 100.53 | 102.18 | 98.76 | 100.53 | 11.93 |
| AHMp-60 min autoclave | 100.36 | 102.41 | 98.86 | 100.53 | 19.15 |
| AHNp | 100.57 | 102.49 | 101.24 | 100.78 | 18.26 |
| AHNp-30 min autoclave | 100.61 | 102.49 | 101.18 | 100.823 | 18.90 |
| AHNp-60 min autoclave | 100.63 | 102.43 | 101.09 | 100.45 | 13.85 |

while the amount of the BSA was significantly enhanced. It indicates that the binding efficiency BSA to all adjuvant samples was not affected by the autoclaving in all given test condition.

The effect of BSA concentration on adsorbed protein was also evaluated (Table 3). It is shown that all samples, both with and without autoclave, still could adsorb maximum BSA portion at BSA feeding concentration of 10 mg/mL. At higher concentration of BSA (20 mg/mL), the adsorption capacity of all adjuvants significantly decreased into lower than 20%. It may be due to the limitation of BSA to access and interact with the surface of adjuvant hindered by the high concentration of BSA itself and the possible increase of the viscosity. This relatively similar adsorption capacity of before and after

autoclave was in accordance with the previous study that elucidate the effect of autoclave of aluminum hydroxide and aluminum phosphate [8].

## 4 Conclusion

Both AHMp and AHNp undergo improved degree of crystallinity after autoclave. This result, however, did not significantly affect their protein adsorption capacity.

**Acknowledgement.** This research was financially supported by INSINAS research fund 2021. We thank to Pharmaceutical and Medical Technology Laboratory-LAPTIAB BPPT for supporting whole experiment and Advanced characterization laboratory – BRIN for providing us XRD analysis using PANalytical AERIS.

## References

1. Hem, S. L.; HogenEsch, H., Relationship between physical and chemical properties of aluminum-containing adjuvants and immunopotentiation. *Expert Rev. Vaccines* **2007,** *6* (5), 685-698.
2. Gupta, R. K., Aluminum compounds as vaccine adjuvants. *Adv. Drug Del. Rev.* **1998,** *32* (3), 155-172.
3. Ruwona, T. B.; Xu, H.; Li, X.; Taylor, A. N.; Shi, Y.-c.; Cui, Z., Toward understanding the mechanism underlying the strong adjuvant activity of aluminum salt nanoparticles. *Vaccine* **2016,** *34* (27), 3059-3067.
4. El Muttaqien, S.; Mardiyati, E.; Rahmani, S., Intraperitoneal acute toxicity of aluminum hydroxide nanoparticles as an adjuvant vaccine candidate in mice. *J Pharmacol Toxicol* **2020,** *15*, 22-35.
5. Pambudi, S.; Mardliyati, E.; Rahmani, S.; Setyawati, D. R.; Widayanti, T.; Gill, A.; Sulfianti, A.; Lestari, W., The Potency of Aluminum Hydroxide Nanoparticles for Dengue Subunit Vaccine Adjuvant. *Microbiology Indonesia* **2018,** *12* (3), 99-105.
6. Hem, S. L.; Johnston, C. T., Production and Characterization of Aluminum-Containing Adjuvants. In *Vaccine Development and Manufacturing, Volume 5 of Wiley Series in Biotechnology and Bioengineering*, John Wiley & Sons, 2014: 2015; Vol. 5, p 319.
7. Art, J.-F.; vander Straeten, A.; Dupont-Gillain, C. C., NaCl strongly modifies the physicochemical properties of aluminum hydroxide vaccine adjuvants. *Int. J. Pharm.* **2017,** *517* (1–2), 226–233.
8. Burrell, L. S.; Lindblad, E. B.; White, J. L.; Hem, S. L., Stability of aluminium-containing adjuvants to autoclaving. *Vaccine* **1999,** *17* (20-21), 2599-2603.
9. Mardliyati, E.; Setyawati, D. R.; Pambudi, S.; Suryandaru; Kusumaningrum, R.; Amal, M. I., Preparation of Aluminum Hydroxide by Precipitation Method for Vaccine Adjuvant Application. *International Journal of Engineering Research and Applications (IJERA)* **2017,** *7* (11), 21–25.
10. Jones, L. S.; Peek, L. J.; Power, J.; Markham, A.; Yazzie, B.; Middaugh, C. R., Effects of adsorption to aluminum salt adjuvants on the structure and stability of model protein antigens. *J. Biol. Chem.* **2005,** *280* (14), 13406-13414.

11. Li, X.; Aldayel, A. M.; Cui, Z., Aluminum hydroxide nanoparticles show a stronger vaccine adjuvant activity than traditional aluminum hydroxide microparticles. *J. Control. Release* **2014,** *173*, 148-157.
12. Li, X.; Hufnagel, S.; Xu, H.; Valdes, S. A.; Thakkar, S. G.; Cui, Z.; Celio, H., Aluminum (oxy) hydroxide nanosticks synthesized in bicontinuous reverse microemulsion have potent vaccine adjuvant activity. *ACS Appl. Mater. Interfaces* **2017,** *9* (27), 22893-22901.
13. Orr, M. T.; Khandhar, A. P.; Seydoux, E.; Liang, H.; Gage, E.; Mikasa, T.; Beebe, E. L.; Rintala, N. D.; Persson, K. H.; Ahniyaz, A., Reprogramming the adjuvant properties of aluminum oxyhydroxide with nanoparticle technology. *npj Vaccines* **2019,** *4* (1), 1.
14. Sun, B.; Ji, Z.; Liao, Y.-P.; Chang, C. H.; Wang, X.; Ku, J.; Xue, C.; Mirshafiee, V.; Xia, T., Enhanced Immune adjuvant activity of aluminum oxyhydroxide nanorods through cationic surface functionalization. *ACS Appl. Mater. Interfaces* **2017,** *9* (26), 21697-21705.
15. Sun, B.; Ji, Z.; Liao, Y.-P.; Wang, M.; Wang, X.; Dong, J.; Chang, C. H.; Li, R.; Zhang, H.; Nel, A. E., Engineering an effective immune adjuvant by designed control of shape and crystallinity of aluminum oxyhydroxide nanoparticles. *ACS nano* **2013,** *7* (12), 10834-10849.
16. Shardlow, E.; Mold, M.; Exley, C., From stock bottle to vaccine: elucidating the particle size distributions of aluminum adjuvants using dynamic light scattering. *Front Chem* **2017,** *4*, 48.
17. He, P.; Zou, Y.; Hu, Z., Advances in aluminum hydroxide-based adjuvant research and its mechanism. *Hum. Vaccines Immunother.* **2015,** *11* (2), 477-488.
18. Shirodkar, S.; Hutchinson, R. L.; Perry, D. L.; White, J. L.; Hem, S. L., Aluminum compounds used as adjuvants in vaccines. *Pharm. Res.* **1990,** *7* (12), 1282-1288.
19. Hem, J.; Roberson, C., Form and stability of aluminum hydroxide complexes in aqueous solution. *US Geological Survey Water-Supply Paper* **1967**.